

# Automatic morphometric extraction of the rabbit osteocytic lacunae using Segment.ai

Osteocytes form an intercellular network similar to a neuronal network in bone. Drs. Tadahiro Iimura and Takanori Sato at the Department of Pharmacology, Faculty of Dental Medicine, Hokkaido University, visualize and measure this network structure, the functional significance of which remains to be elucidated. Since osteocytes have a structure that is continuous with osteocytic processes (countless cellular processes protruding from the cell body), extracting the morphologies of individual cells using the conventional fluorescence binarization method is a tall order. In this application note, we introduce an example of the use of Segment.ai, one of the functions of the NIS.ai module for microscopes, to automate segmentation of osteocytic lacunae in order to facilitate measurement of their numbers and morphology.

## Research background

Bone is composed of three types of cells: bone-forming osteoblasts, bone-resorbing osteoclasts, and mechano-sensing osteocytes. Bone homeostasis is maintained by the coordinated actions of these cells. Bone is constantly being remodeled, maintaining a dynamic equilibrium, but if the balance is lost, diseases such as osteoporosis can occur. Osteocytes make up a very dense intercellular network in hard bone (Fig. 1). This network is very diverse and can be associated with the degree of load on the bone and bone turnover (the turnover rate of formation and destruction), but many points are still unclear.

## Experiment overview

Measurement of the number and morphology of osteocytes is an important indicator for exploring the metabolic pathophysiology of bone. Professor Iimura et al. revealed that the network of osteocytic lacunae (bone cavities surrounding osteocytes) and osteocytic canaliculi (bone cavities that encase osteocytic processes) can be visualized by auto-fluorescence using a confocal microscope (Fig. 1, Reference). Conventional binarization methods require additional manual adjustment to distinguish osteocytic lacunae from osteocytic canaliculi, which have continuous structures and intensity values (Fig. 2b). By applying Segment.ai to the acquired images, we succeeded in automatically extracting the morphologies of osteocytic lacunae (Fig. 2c).

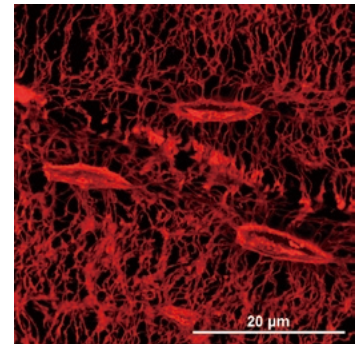


Fig. 1: Network of osteocytic lacunae-canalicular system

Auto-fluorescence imaging of Villanueva-stained rabbit tibia. This image was taken as a Z stack with a resolution of 0.04  $\mu\text{m}/\text{pixel}$  using a 100X objective, subjected to enhanced resolution processing, and displayed as a maximum intensity projection (MIP). Scale bar: 20  $\mu\text{m}$

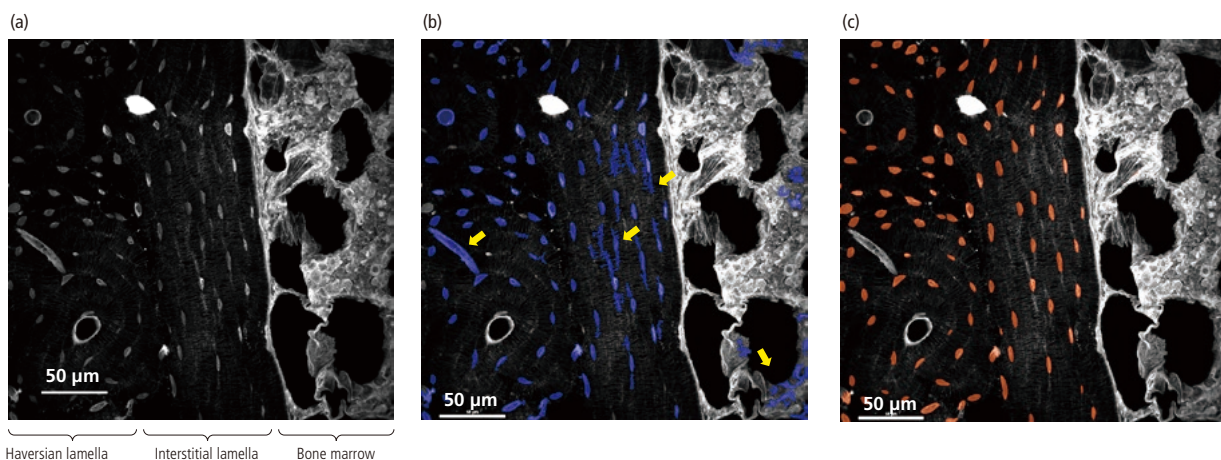


Fig. 2: Comparison of automatic segmentation by the conventional binarization method (b) and Segment.ai (c)

Villanueva-stained un-decalcified bone section of a rabbit was excited with 561 nm to detect auto-fluorescence using a confocal microscope. The image was taken as a Z stack using a 60X objective and displayed as a MIP. Scale bar: 50  $\mu\text{m}$

(a) The observed bone tissue is histologically composed of Haversian lamella, interstitial lamella and bone marrow.

(b) Results of segmentation by the conventional binarization method (blue). Structures other than osteocytic lacunae, such as osteocytic canaliculi and some parts of bone marrow, were detected (arrows). Manual mask modification or removal is required for accurate measurement.

(c) Results of segmentation using Segment.ai (orange). Only the osteocytic lacunae were fully detected by Segment.ai, which learned how to identify osteocytic lacuna areas.

Segment.ai workflow consists of 3 steps (Fig. 3). Training datasets contain an expected image that has been manually binarized, and input image data prior to binarization.

The critical parameter for the accuracy of Segment.ai is the number of images of the training data. In this experiment, we firstly captured multiple parts of the bone section to increase the image variation. Then, these images were used for training data. For training, we created four types of data sets with different numbers of images, such as 1, 4, 15, and 20, and evaluated the success rate of Segment.ai that has learned using these data sets.

As a result, it was clarified that by training Segment.ai using more than 15 training images, automatic extraction of osteocytic lacunae could be achieved with 95% accuracy (Fig. 4).

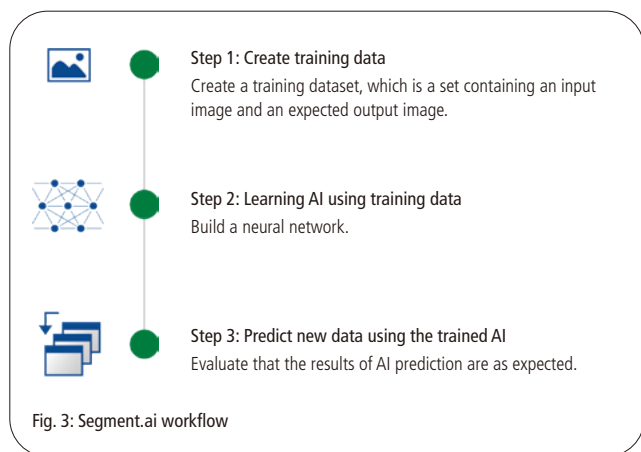


Fig. 3: Segment.ai workflow

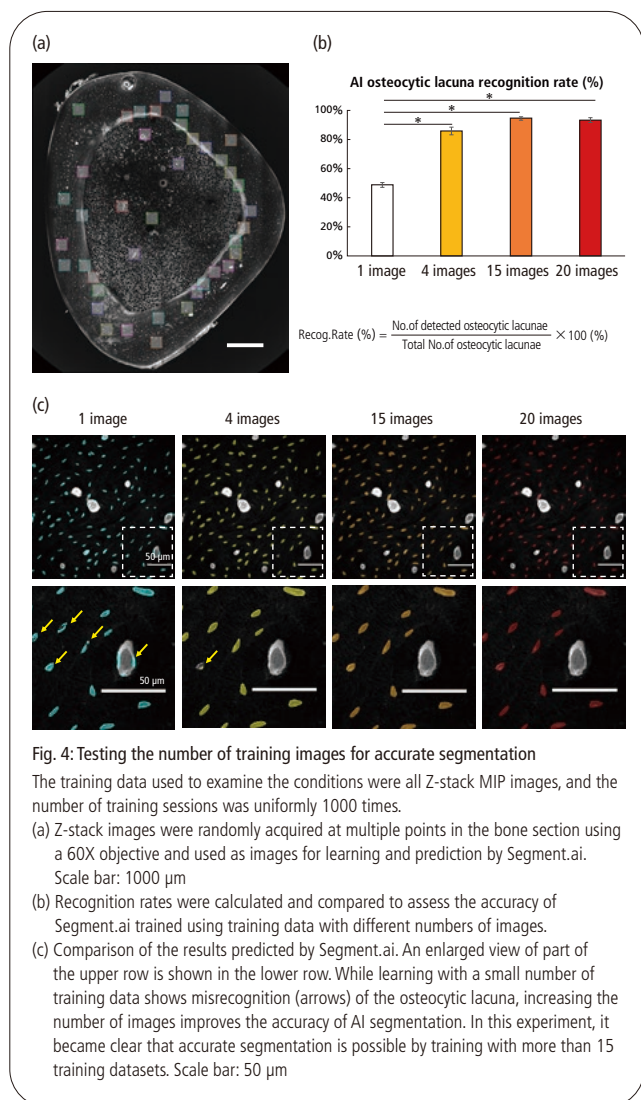


Fig. 4: Testing the number of training images for accurate segmentation

The training data used to examine the conditions were all Z-stack MIP images, and the number of training sessions was uniformly 1000 times.

(a) Z-stack images were randomly acquired at multiple points in the bone section using a 60X objective and used as images for learning and prediction by Segment.ai. Scale bar: 1000  $\mu\text{m}$

(b) Recognition rates were calculated and compared to assess the accuracy of Segment.ai trained using training data with different numbers of images.

(c) Comparison of the results predicted by Segment.ai. An enlarged view of part of the upper row is shown in the lower row. While learning with a small number of training data shows misrecognition (arrows) of the osteocytic lacuna, increasing the number of images improves the accuracy of AI segmentation. In this experiment, it became clear that accurate segmentation is possible by training with more than 15 training datasets. Scale bar: 50  $\mu\text{m}$

## Summary

Bone morphometry, which is the standard method for bone tissue analysis, requires highly elaborate skills for manual measurement of the acquired brightfield image of a bone section. Even when performing automatic recognition by binarizing the intensity value in a fluorescent image, manual work was required for accurate segmentation. The use of Segment.ai eliminates the need for manual segmentation and allows objective evaluation instead of subjective analysis (Fig. 5). Anyone can perform accurate analysis of a large amount of data in a bias-free and highly effective way (References 1, 2).

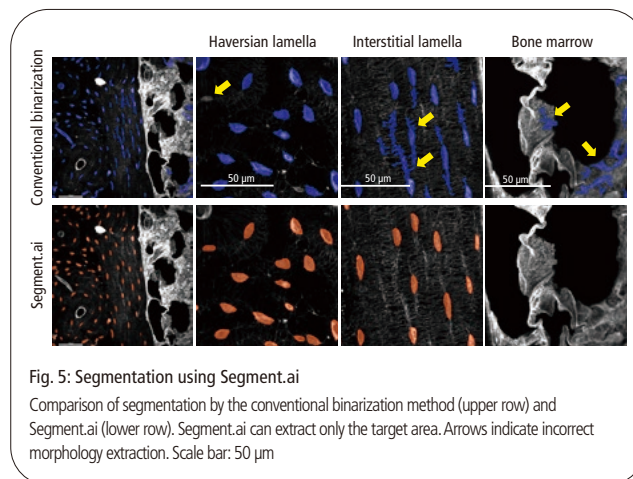


Fig. 5: Segmentation using Segment.ai

Comparison of segmentation by the conventional binarization method (upper row) and Segment.ai (lower row). Segment.ai can extract only the target area. Arrows indicate incorrect morphology extraction. Scale bar: 50  $\mu\text{m}$

## Reference

1. Takanori Sato, Aya Takakura, Ji-Won Lee, Kazuaki Tokunaga, Haruka Matsumori, Ryoko Takao-Kawabata, Tadahiro Iimura *Microscopy* (Oxf). 2021 Jun 8; dfab020
2. Aya Takakura, Takanori Sato, Ji-Won Lee, Kyoko Hirano, Ryoko Takao-Kawabata, Toshinori Ishizuya, Tadahiro Iimura *Scientific Reports*, Volume 12, Article number: 16799 (2022)

## Product Information

### AX/AX R Confocal Microscope

These microscopes achieve high resolution images of 8K x 8K pixels, which is four times that of conventional models. A large FOV with a diagonal of 25 mm allows acquisition of a large area of samples in a single scan, reducing phototoxicity. The AX R's resonant scanner achieves a high resolution of 2K x 2K pixels, allowing acquisition of live sample dynamics with high-speed imaging of up to 720 fps (2048 x 16 pixels).



### NIS.ai AI Module for Microscopes

NIS.ai is an image processing and analysis module that extends the capabilities of the NIS-Elements imaging software, and includes Enhance.ai, Convert.ai, and Segment.ai. Segment.ai provides a new solution for target extraction, which is difficult or requires manual adjustment in traditional binarization.

